

CONVOLUTION QUADRATURES BASED ON BLOCK GENERALIZED ADAMS METHODS *

LING LIU[†] AND JUNJIE MA[‡]

Abstract. This paper studies a family of convolution quadratures, a numerical technique for efficient evaluation of convolution integrals. We employ the block generalized Adams method to discretize the underlying initial value problem, departing from the well-established approaches that rely on linear multistep formulas or Runge-Kutta methods. The convergence order of the proposed convolution quadrature can be dynamically controlled without requiring grid point adjustments, enhancing flexibility. Through strategic selection of the local interpolation polynomial and block size, the method achieves high-order convergence for calculation of convolution integrals with hyperbolic kernels. We provide a rigorous convergence analysis for the proposed convolution quadrature and numerically validate our theoretical findings for various convolution integrals.

Key words. Convolution quadrature; Convolution integral; Block generalized Adams method; Convergence analysis; Integral equation.

AMS subject classifications. 65D32, 65R10

1. Introduction. Convolution integrals (CIs) have a number of applications in computational practice, such as time-domain boundary integral equations [5], Volterra integral equations of convolution-type [10], fractional differential equations [4, 17, 28] and Maxwell's equations [30]. In this paper, we investigate the numerical evaluation of the following CI

$$(1.1) \quad \int_0^t k(s)g(t-s)ds \quad \text{with } t \in [0, T],$$

where g is a given smooth function. When the kernel function k itself is known previously, many efficient approaches can be used to compute CI (1.1), for example, the convolution spline method [12] and spectral method based on orthogonal polynomial convolution matrices [31, 32]. However, if the Laplace transform K of the kernel function k is known, then the convolution quadrature (CQ), which was proposed by Lubich (see [20, 21, 23]), becomes an attractive choice due to its suitability for stable integration over long time intervals.

For clarity, we introduce the following notation to represent CI (1.1) (see also [2]),

$$(1.2) \quad (K(\partial_t)g)(t) := \int_0^t k(s)g(t-s)ds \quad \text{with } t \in [0, T].$$

Here we have $(\partial_t^{-1}g)(t) = \int_0^t g(s)ds$ and $(\partial_t g)(t) = g'(t) + g(0)\delta(t)$ with δ denoting Dirac delta function. Noting that

$$(1.3) \quad k(s) = \frac{1}{2\pi i} \int_{\Gamma} K(\lambda)e^{\lambda s}d\lambda \quad \text{with } s > 0,$$

*This work was supported by National Natural Science Foundation of China (No. 11901133) and Training Program of Guizhou University (No. GDPY[2020]39).

[†]School of Mathematics and Statistics, Guizhou University, Guiyang, Guizhou 550025, P.R. China.

[‡]School of Mathematics and Statistics, Guizhou University, Guiyang, Guizhou 550025, P.R. China.(jjma@gzu.edu.cn).

where Γ is a carefully chosen contour that falls in the analytic region of K , we can compute

$$(1.4) \quad (K(\partial_t)g)(t) = \frac{1}{2\pi i} \int_{\Gamma} K(\lambda) \int_0^t e^{\lambda s} g(t-s) ds d\lambda.$$

Letting $y(t) = \int_0^t e^{\lambda s} g(t-s) ds$, we obtain the initial value problem (IVP) for the ordinary differential equation (ODE):

$$(1.5) \quad \begin{cases} y'(t) = \lambda y(t) + g(t) & \text{with } t > 0, \\ y(0) = 0. \end{cases}$$

The calculation of CI (1.2) then consists of two steps: approximating IVP (1.5) using time-stepping methods, and computing contour integrals.

The literature boasts extensive research on two primary types of ODE solvers for IVP (1.5). Lubich's pioneering work in [20, 21] established the foundation for the linear multistep convolution quadrature (LMCQ) by applying linear multistep formulas for discretization of IVP (1.5). Convergence analysis revealed that LMCQ achieves the same convergence order as the underlying linear multistep formula, but only after adding correction terms. LMCQ is implemented on a uniform grid and offers the advantage of adjusting its convergence order without modifying the grid points. This implies changing the convergence order of LMCQ does not need to re-evaluate g , since evaluating the function g depends solely on the grid points. This advantage extends to adaptive algorithms as well. When doubling the grid points, LMCQ can efficiently reuse the previously computed values of g . These combined advantages make LMCQ a compelling choice for a wide range of time-space problems. These problems often involve computationally expensive spatial discretizations, such as those encountered with time-fractional differential operators (see [11, 17]). However, A -stable multistep methods are limited by Dalquist's order barrier to a maximum convergence order of 2. Due to this limitation, LMCQs are typically constructed using lower-order formulas, like the second-order backward difference (BDF2) [11] or the trapezoid rule (TR) [7, 13], to guarantee A -stability when applied to hyperbolic problems. In contrast, Runge-Kutta methods can achieve A -stability for any desired order by strategically selecting non-uniform stage nodes, such as Gauss-Legendre, Radau or Lobatto points [2, 6]. Therefore, CQ based on Runge-Kutta method (RKCQ) can provide arbitrarily high-order and stable approximations to CI (1.2) with a hyperbolic kernel (see [2]). Benefitting from its excellent stability, high-order RKCQ offers a broader range of applications compared to LMCQ. This is particularly advantageous for numerical studies of the wave equation (see [5, 24, 25, 27]). In addition, recent studies also demonstrate numerous modifications to the original CQs, including fast implementation techniques [1, 3, 14], variable time stepping strategies [7, 18, 19] and efficient computation of highly oscillatory integrals [26].

The aim of this paper is to develop a family of CQs that combines the strengths of LMCQs and RKCQs: It is implemented on the uniform grid and offers the flexibility to adjust the convergence order without requiring additional grid points as LMCQ does; The proposed method can achieve high-order and stable calculation of CI (1.2) with a hyperbolic kernel as RKCQ does. This is achieved by leveraging the block generalized Adams method (BGA) as the foundation for the underlying ODE solvers, which draws inspiration from the application of the boundary value method in the numerical solutions of ODEs (see [8, 15, 16]). Henceforth, we suppose that $K(\lambda)$ is

analytic in the half-plane

$$\mathbb{C}_\sigma := \{z \in \mathbb{C} : \operatorname{Re}(z) \geq \sigma\} \quad \text{with } \sigma \in \mathbb{R},$$

and bounded as $|K(\lambda)| \leq M|\lambda|^\mu$ within \mathbb{C}_σ for a positive constant M and a real number μ .

The remainder of the paper is structured as follows. Section 2 introduces BGA for IVP (1.5). Building upon BGA, Section 3 develops the BGA-based convolution quadrature (BGACQ). We then analyze BGACQ's convergence properties under hypotheses of regularity. Section 4 presents numerical experiments to verify the proposed quadrature rule's convergence and stability.

2. BGA for IVP (1.5). This section introduces the ODE solver, BGA, for IVP (1.5) and explores several BGAs which can be employ in the formulation of CQ for CI with a hyperbolic kernel.

To begin with, we define the uniform coarse grid, denoted by \mathcal{X}_N ,

$$\mathcal{X}_N := \{\tau_n := nh, n = 0, 1, \dots, N\},$$

where $h = T/N$ represents the grid step size. Within each subinterval $[\tau_n, \tau_{n+1}]$, we introduce a uniform fine grid that plays a role analogous to the stages in a Runge-Kutta method,

$$\mathbf{X}_m^n := \{t_j^n := \tau_n + jh/m, j = 0, 1, \dots, m\}.$$

It can be easily examined that $t_0^n = \tau_n$ and $t_m^n = \tau_{n+1}$. For $j = 0, 1, \dots, m-1$, integration of both sides of IVP (1.5) from t_j^n to t_{j+1}^n gives

$$(2.1) \quad y(t_{j+1}^n) - y(t_j^n) = \int_{t_j^n}^{t_{j+1}^n} (\lambda y(s) + g(s)) ds = \int_{t_j^n}^{t_{j+1}^n} f(s) ds,$$

where $f(s) := \lambda y(s) + g(s)$.

Next, define the piecewise polynomial space by

$$S_m(\mathbf{X}_m^n) := \{v \in C[\tau_n, \tau_{n+1}] : v|_{[t_j^n, t_{j+1}^n]} \in \pi_m, j = 0, 1, \dots, m-1\},$$

where $C[\tau_n, \tau_{n+1}]$ comprises continuous functions over the interval $[\tau_n, \tau_{n+1}]$, and $v|_{[t_j^n, t_{j+1}^n]} \in \pi_m$ indicates v is a polynomial with its degree not exceeding m over the subinterval $[t_j^n, t_{j+1}^n]$. Given any nonnegative integers k_1 and k_2 , we further define the local fundamental functions

$$\phi_i^{k_1, k_2}(v) = \prod_{l=-k_1, l \neq i}^{k_2+1} \frac{v-l}{i-l} \quad \text{with } i = -k_1, \dots, k_2+1.$$

Then we denote \mathcal{P}_m^n as an interpolation operator acting on functions in $C[\tau_n, \tau_{n+1}]$, mapping them to the space of $S_m(\mathbf{X}_m^n)$. When $s \in [t_j^n, t_{j+1}^n]$ with $j = k_1, k_1+1, \dots, m-k_2-1$, we define $\mathcal{P}_m^n[f]$ as

$$\mathcal{P}_m^n[f](s) = \mathcal{P}_m^n[f](t_j^n + vh/m) := \sum_{i=-k_1}^{k_2+1} f(t_{j+i}^n) \phi_i^{k_1, k_2}(v), \quad v \in [0, 1].$$

To ensure the solvability of the resulting discretization, we employ an “additional method” over the initial interval $[t_0^n, t_{k_1}^n]$ and the final interval $[t_{m-k_2}^n, t_m^n]$, similar to the approach used in block boundary value methods (see [8, pp.283]). When $s \in [t_0^n, t_{k_1}^n]$, we define $\mathcal{P}_m^n[f]$ as

$$\mathcal{P}_m^n[f](s) = \mathcal{P}_m^n[f](t_{k_1}^n + vh/m) := \sum_{i=-k_1}^{k_2+1} f(t_{k_1+i}^n) \phi_i^{k_1, k_2}(v),$$

where $v \in [-k_1, 0]$. When $s \in [t_{m-k_2}^n, t_m^n]$, we define $\mathcal{P}_m^n[f]$ as

$$\mathcal{P}_m^n[f](s) = \mathcal{P}_m^n[f](t_{m-k_2-1}^n + vh/m) := \sum_{i=-k_1}^{k_2+1} f(t_{m-k_2-1+i}^n) \phi_i^{k_1, k_2}(v),$$

where $v \in [1, k_2 + 1]$. For $i = -k_1, \dots, k_2 + 1$, define the notations

$$\begin{aligned} \alpha_i &:= \frac{1}{m} \int_0^1 \phi_i^{k_1, k_2}(v) dv, \\ \alpha_i^{(j)} &:= \frac{1}{m} \begin{cases} \int_{j-k_1}^{j-k_1+1} \phi_i^{k_1, k_2}(v) dv, & j = 0, \dots, k_1 - 1, \\ \int_{j-m+k_2+1}^{j-m+k_2+2} \phi_i^{k_1, k_2}(v) dv, & j = m - k_2, \dots, m - 1. \end{cases} \end{aligned}$$

This yields the quadrature rule $Q_j^n[f] := \int_{t_j^n}^{t_{j+1}^n} \mathcal{P}_m^n[f](s) ds$ for the integral $\int_{t_j^n}^{t_{j+1}^n} f(s) ds$, that is,

$$(2.2) \quad Q_j^n[f] = h \sum_{i=-k_1}^{k_2+1} \begin{cases} f(t_{k_1+i}^n) \alpha_i^{(j)}, & j = 0, \dots, k_1 - 1, \\ f(t_{j+i}^n) \alpha_i, & j = k_1, \dots, m - k_2 - 1, \\ f(t_{m-k_2-1+i}^n) \alpha_i^{(j)}, & j = m - k_2, \dots, m - 1. \end{cases}$$

Before delving into the discretization of IVP (1.5), let's examine the quadrature error q_j^n defined by

$$q_j^n := \int_{t_j^n}^{t_{j+1}^n} (\mathcal{I} - \mathcal{P}_m^n)[f](s) ds,$$

where \mathcal{I} denotes the identity transformation. In fact, the Peano kernel theorem [9, pp. 43] allows us to quantify the difference between the exact function f and its approximate piecewise polynomial $\mathcal{P}_m^n[f]$ over the subinterval $[t_j^n, t_{j+1}^n]$. Denote

$$\mathcal{E}_j^n(s) := \int_{-k_1}^{k_2+1} \kappa(s, v) f^{(k_1+k_2+2)}(t_j^n + vh/m) dv, \quad j = k_1, \dots, m - k_2 - 1,$$

where $f^{(k_1+k_2+2)}(t_j^n + vh/m)$ represents the $(k_1 + k_2 + 2)$ -th order derivative of $f(t)$ at $t_j^n + vh/m$, and the kernel $\kappa(s, v)$ is defined by

$$\kappa(s, v) := \frac{1}{(p-1)!} \left((s-v)_+^{k_1+k_2+1} - \sum_{i=-k_1}^{k_2+1} \phi_i^{k_1, k_2}(s) (i-v)_+^{k_1+k_2+1} \right)$$

with $(s - v)_+ := 0$ for $s < v$ and $(s - v)_+ := s - v$ for $s \geq v$. In the case of $j = 0, \dots, k_1 - 1$, letting $t = t_{k_1}^n + sh/m$, we represent the remainder $(\mathcal{I} - \mathcal{P}_m^n)[f](t)$ in the form of

$$(\mathcal{I} - \mathcal{P}_m^n)[f](t_{k_1}^n + sh/m) = \frac{h^{k_1+k_2+2}}{m^{k_1+k_2+2}} \mathcal{E}_{k_1}^n(s), \quad s \in [j - k_1, j - k_1 + 1].$$

When $t \in [t_j^n, t_{j+1}^n]$ with $j = k_1, \dots, m - k_2 - 1$, letting $t = t_j^n + sh/m$, we represent $(\mathcal{I} - \mathcal{P}_m^n)[f](t)$ by

$$(\mathcal{I} - \mathcal{P}_m^n)[f](t_j^n + sh/m) = \frac{h^{k_1+k_2+2}}{m^{k_1+k_2+2}} \mathcal{E}_j^n(s), \quad s \in [0, 1].$$

In the case of $j = m - k_2, \dots, m - 1$, letting $t = t_{m-k_2-1}^n + sh/m$, for $s \in [j - m + k_2 + 1, j - m + k_2 + 2]$, the approximation error is represented by

$$(\mathcal{I} - \mathcal{P}_m^n)[f](t_{m-k_2-1}^n + sh/m) = \frac{h^{k_1+k_2+2}}{m^{k_1+k_2+2}} \mathcal{E}_{m-k_2-1}^n(s).$$

Consequently, the quadrature error q_j^n is expressed as

$$(2.3) \quad q_j^n = \frac{h^{k_1+k_2+3}}{m^{k_1+k_2+3}} \begin{cases} \int_{j-k_1}^{j-k_1+1} \mathcal{E}_j^n(s) ds, & j = 0, \dots, k_1 - 1, \\ \int_0^1 \mathcal{E}_j^n(s) ds, & j = k_1, \dots, m - k_2 - 1, \\ \int_{j-m+k_2+1}^{j-m+k_2+2} \mathcal{E}_j^n(s) ds, & j = m - k_2, \dots, m - 1. \end{cases}$$

We let the curve Γ to be $\sigma + i\mathbb{R}$ and introduce the assumption on the function g :

$$g(0) = g'(0) = \dots = g^{(k_1+k_2+1)}(0) = 0.$$

This assumption will hold throughout the following discussion unless explicitly stated otherwise. Noting that

$$y(t) = \int_0^t e^{\lambda s} g(t-s) ds \quad \text{and} \quad f(t) = \lambda y(t) + g(t),$$

we obtain through a straightforward calculation

$$(2.4) \quad f^{(k_1+k_2+2)}(t) = \lambda \int_0^t g^{(k_1+k_2+2)}(t-s) e^{\lambda s} ds + g^{(k_1+k_2+2)}(t).$$

Since $\int_0^t g^{(k_1+k_2+2)}(t-s) e^{\lambda s} ds$ becomes highly oscillatory when $\lambda \in \Gamma$ and $|\lambda| > 1$, we derive according to van der Corput lemma [29, pp.332],

$$\|f^{(k_1+k_2+2)}\| \leq C \quad \text{for any } \lambda \in \Gamma,$$

where $\|\cdot\|$ denotes the maximum norm. Throughout the following analysis, C represents a generic positive constant that does not depend on λ or h . It follows from Eq. (2.3) that

$$|q_j^n| \leq Ch^{k_1+k_2+3} \quad \text{for any } \lambda \in \Gamma.$$

LEMMA 2.1. *Assume the function g in CI (1.2) possesses a continuous derivative of order at least $k_1 + k_2 + 2$ over $[0, T]$, and satisfies the condition*

$$g(0) = g'(0) = \dots = g^{(k_1+k_2+1)}(0) = 0.$$

TABLE 2.1
Numerical approximations to eigenvalues of $\mathbf{A}^{-1}\mathbf{L}$.

	$m = m^*$	$m = 12$
$(k_1, k_2) = (0, 1)$	5.5, $3.6 \pm 2.8i$	$19 \pm 2.1i$, $18 \pm 5.9i$, $11 \pm 12i$, $12 \pm 11i$, $16 \pm 8.7i$, $13 \pm 11i$
$(k_1, k_2) = (0, 2)$	$5.7 \pm 1.1i$, $3.3 \pm 4.9i$,	$5.7 \pm 14i$, $7.6 \pm 14i$, $10 \pm 12i$, $12 \pm 8.4i$, $13 \pm 4.4i$, $13 \pm 1.0i$
$(k_1, k_2) = (1, 2)$	$3.7 \pm 7.0i$, 7.8, $6.3 \pm 2.9i$	$8.2 \pm 17i$, $10 \pm 15i$, $13 \pm 13i$, $15 \pm 8.7i$, $15 \pm 5.1i$, $16 \pm 1.8i$

To ensure the resulting CQ can handle CI (1.2) with a hyperbolic kernel, we introduce the following assumption regarding the ODE solver.

ASSUMPTION 2.1. *Suppose the stability function of BGA is defined as $R_m(z) = \mathbf{e}_m^T(\mathbf{L} - z\mathbf{A})^{-1}(z\mathbf{a} - \mathbf{1})$, and the following statement holds true:*

- \mathbf{A} is invertible, and all eigenvalues of $\mathbf{A}^{-1}\mathbf{L}$ are positive;
- $|R_m(i\omega)| < 1$, $\omega \neq 0$;
- $|R_m(\infty)| = |\mathbf{e}_m^T\mathbf{A}^{-1}\mathbf{a}| < 1$.

The first condition implies that $\mathbf{L} - z\mathbf{A}$ is invertible for all $z \in \mathbb{C}^-$. Consequently, $R_m(z)$ is analytic within this half-plane. Since $R_m(0) = 1$, the second condition guarantees that $|R_m(z)| \leq 1$ holds for all $z \in \mathbb{C}^-$ according to the maximum-modulus principle. Therefore, these first two conditions together ensure that the corresponding BGA is A -stable. From a numerical implementation standpoint, the second condition can be relaxed to $|R_m(i\omega)| \leq 1$ for $\omega \in \mathbb{R}$. The modified second condition and the third condition play a twofold role: they simplify the convergence order proof and ensure the corresponding ODE solver can solve stiff problems more efficiently compared to solvers where $|R_m(\infty)| = 1$. Table 2.1 summarizes the approximate eigenvalues of $\mathbf{A}^{-1}\mathbf{L}$ for several BGAs with $m^* = k_1 + k_2 + 2$. The numerical experiments suggest that all eigenvalues of $\mathbf{A}^{-1}\mathbf{L}$ seem to have positive real parts in these cases. In Figure 2.1, we plot the stability boundaries for BGAs. These boundaries represent the curves where $|R_m(z)| = 1$. Because $R_m(z)$ is analytic outside these boundaries, the maximum-modulus principle guarantees that its modulus remains less than or equal to 1 within that region. Based on the numerical results, it seems that these schemes are A -stable. Table 2.2 presents the limits, $|R_m(\infty)|$, for these A -stable methods. As the table shows, all limits are strictly less than 1. Numerical experiments also confirm that this limit approaches 0 as m increases. While arbitrary choices of k_1, k_2 and m don't generally guarantee that BGA satisfies Assumption 2.1, we can identify a minimum block size numerically to ensure this property holds. We list the minimum block size m^* for several BGAs satisfying Assumption 2.1 in Table 2.3, and will not explore the broader range of BGAs that might also satisfy this assumption.

In conclusion, we demonstrate that BGA can be employed to construct a family of A -stable ODE solvers suitable for designing CQs. These BGA-based schemes leverage a uniform grid, eliminating the need for special points required by RK and allowing for adjustment of convergence order without grid point changes. While numerical evidence suggests BGA itself is not L -stable, it exhibits a significantly smaller magnitude of the stability function at infinity compared to conservative schemes. This

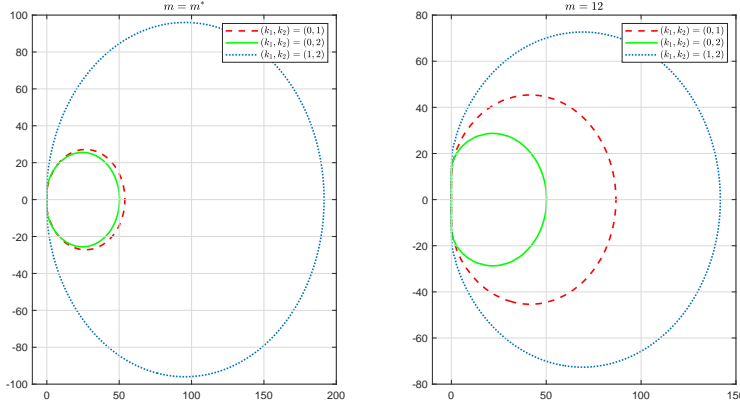


FIG. 2.1. Boundaries of the stability regions for BGAs with $m = m^*$ (left) and $m = 12$ (right).

TABLE 2.2
 $|\mathbf{R}_m(\infty)|$ for various A -stable BGAs.

m	m^*	12	24	48
$(k_1, k_2) = (0, 1)$	5.9×10^{-1}	4.5×10^{-3}	6.9×10^{-6}	1.6×10^{-11}
$(k_1, k_2) = (0, 2)$	4.3×10^{-2}	4.4×10^{-4}	1.4×10^{-8}	1.5×10^{-17}
$(k_1, k_2) = (1, 2)$	7.4×10^{-1}	7.6×10^{-2}	1.5×10^{-3}	6.3×10^{-7}

characteristic, similar to L -stable RKCQs, makes CQ based on BGA less susceptible to issues like spurious oscillations, as discussed in [1]. Compared to RK, increasing the block size of BGA offers a significant advantage due to the Toeplitz-like structure of \mathbf{A} . This allows us to easily capture global information using relatively large time steps, as demonstrated in [8, pp.289].

3. BGACQ for CI (1.2). This section explores the application of BGA to construct a family of CQs for computing CI (1.2) with a hyperbolic kernel. We will also analyze the convergence property of this method.

Multiplying both sides of Eq. (2.5) by ζ^n and doing summation over n from 0 to ∞ give

$$(3.1) \quad (\mathbf{L} - h\lambda\mathbf{A})\mathbf{Y}(\zeta) = \zeta(h\lambda\mathbf{a} - \mathbf{I})\mathbf{e}_m^T\mathbf{Y}(\zeta) + h(\mathbf{A} + \zeta\mathbf{a}\mathbf{e}_m^T)\mathbf{G}(\zeta),$$

where $\mathbf{Y}(\zeta) = \sum_{n=0}^{\infty} \mathbf{Y}_n\zeta^n$, $\mathbf{G}(\zeta) = \sum_{n=0}^{\infty} \mathbf{G}_n\zeta^n$. A direct calculation leads to

$$(3.2) \quad ((\mathbf{L} + \zeta\mathbf{l}\mathbf{e}_m^T) - h\lambda(\mathbf{A} + \zeta\mathbf{a}\mathbf{e}_m^T))\mathbf{Y}(\zeta) = h(\mathbf{A} + \zeta\mathbf{a}\mathbf{e}_m^T)\mathbf{G}(\zeta).$$

Since the spectral radius of $\mathbf{A}^{-1}\mathbf{a}\mathbf{e}_m^T$ equals to $|\mathbf{e}_m^T\mathbf{A}^{-1}\mathbf{a}| = |\mathbf{R}_m(\infty)|$, it follows from Assumption 2.1 that $\mathbf{A} + \zeta\mathbf{a}\mathbf{e}_m^T = \mathbf{A}(\mathbf{E}_m + \zeta\mathbf{A}^{-1}\mathbf{a}\mathbf{e}_m^T)$ is invertible for $|\zeta| < 1$. We can now safely define the discretized differential symbol $\Delta(\zeta)$ for BGA as

$$\Delta(\zeta) := (\mathbf{A} + \zeta\mathbf{a}\mathbf{e}_m^T)^{-1}(\mathbf{L} + \zeta\mathbf{l}\mathbf{e}_m^T).$$

Then Eq. (3.2) turns to

$$(3.3) \quad (\Delta(\zeta)/h - \lambda\mathbf{E}_m)\mathbf{Y}(\zeta) = \mathbf{G}(\zeta),$$

TABLE 2.3
Minimum block size m^* for BGA satisfying Assumption 2.1.

(k_1, k_2)	(0, 1)	(0, 2)	(1, 2)	(1, 3)	(2, 3)	(2, 4)	(3, 4)	(3, 5)
m^*	3	4	5	6	7	10	13	13

where \mathbf{E}_m denotes the $m \times m$ identity matrix.

The next step is to prove that all eigenvalues of the matrix $\Delta(\zeta)$ with $|\zeta| < 1$ lie in the complex half-plane \mathbb{C}^+ . This is equivalent to demonstrating that $\Delta(\zeta) - z\mathbf{E}_m$ is invertible for all $z \in \mathbb{C}^-$ and $|\zeta| < 1$. In fact, we can establish a more rigorous result, as shown below.

LEMMA 3.1. *Suppose that BGA satisfies Assumption 2.1, $\Delta(\zeta)$ is its discretized differential symbol, and its stability domain, \mathbb{D} , is denoted by*

$$\mathbb{D} := \{z \in \mathbb{C} : |\mathbf{R}_m(z)| \leq 1\}.$$

Then for any $z \in \mathbb{D}$ and $|\zeta| < 1$, $\Delta(\zeta) - z\mathbf{E}_m$ is invertible and its inverse can be represented by

$$\begin{aligned} (\Delta(\zeta) - z\mathbf{E}_m)^{-1} &= (\mathbf{L} - z\mathbf{A})^{-1}\mathbf{A} + \mathbf{R}_m(z)\mathbf{B}(\mathbf{L} - z\mathbf{A})^{-1}\mathbf{A}\zeta \\ &\quad + \sum_{j=2}^{\infty} ((\mathbf{R}_m(z))^j\mathbf{B}(\mathbf{L} - z\mathbf{A})^{-1}\mathbf{A} + (\mathbf{R}_m(z))^{j-1}\mathbf{B}(\mathbf{L} - z\mathbf{A})^{-1}\mathbf{a}\mathbf{e}_m^T)\zeta^j, \end{aligned}$$

where $\mathbf{B} := (\mathbf{L} - z\mathbf{A})^{-1}(z\mathbf{a} - \mathbf{l})\mathbf{e}_m^T$.

Proof. Direct computation implies for any $z \in \mathbb{D}$,

$$\begin{aligned} \Delta(\zeta) - z\mathbf{E}_m &= (\mathbf{A} + \zeta\mathbf{a}\mathbf{e}_m^T)^{-1}((\mathbf{L} + \zeta\mathbf{l}\mathbf{e}_m^T) - z(\mathbf{A} + \zeta\mathbf{a}\mathbf{e}_m^T)) \\ &= (\mathbf{A} + \zeta\mathbf{a}\mathbf{e}_m^T)^{-1}((\mathbf{L} - z\mathbf{A}) + \zeta(\mathbf{l}\mathbf{e}_m^T - z\mathbf{a}\mathbf{e}_m^T)). \end{aligned}$$

Because all eigenvalues of $\mathbf{A}^{-1}\mathbf{L}$ reside in the domain $\mathbb{C} \setminus \mathbb{D}$, it follows that the matrix $\mathbf{L} - z\mathbf{A}$ is invertible. Consequently, we obtain

$$\Delta(\zeta) - z\mathbf{E}_m = (\mathbf{A} + \zeta\mathbf{a}\mathbf{e}_m^T)^{-1}(\mathbf{L} - z\mathbf{A})(\mathbf{E}_m - \zeta\mathbf{B}).$$

For $j \geq 2$, direct computation yields

$$\mathbf{B}^j = \mathbf{R}_m(z)\mathbf{B}^{j-1} = (\mathbf{R}_m(z))^{j-1}\mathbf{B}.$$

Since $|\mathbf{R}_m(z)| \leq 1$ holds for any $z \in \mathbb{D}$, we get the inequality $|\mathbf{R}_m(z)\zeta| < 1$ for all $|\zeta| < 1$, which implies

$$\|\mathbf{B}\zeta\|^j \leq |\mathbf{R}_m(z)\zeta|^{j-1}\|\mathbf{B}\zeta\| < 1$$

for sufficiently large j . Consequently, the series $\sum_{j=0}^{\infty} (\mathbf{B}\zeta)^j$ is a Neumann series and converges to the inverse of $\mathbf{E}_m - \zeta\mathbf{B}$ in the case of $|\zeta| < 1$. In conclusion, we have established that all eigenvalues of the matrix $\Delta(\zeta)$ lie in the domain $\mathbb{C} \setminus \mathbb{D}$ for $|\zeta| < 1$. Furthermore, it follows by a direct calculation that

$$\begin{aligned} (\Delta(\zeta) - z\mathbf{E}_m)^{-1} &= (\mathbf{L} - z\mathbf{A})^{-1}\mathbf{A} + \mathbf{R}_m(z)\mathbf{B}(\mathbf{L} - z\mathbf{A})^{-1}\mathbf{A}\zeta \\ &\quad + \sum_{j=2}^{\infty} ((\mathbf{R}_m(z))^j\mathbf{B}(\mathbf{L} - z\mathbf{A})^{-1}\mathbf{A} + (\mathbf{R}_m(z))^{j-1}\mathbf{B}(\mathbf{L} - z\mathbf{A})^{-1}\mathbf{a}\mathbf{e}_m^T)\zeta^j. \end{aligned}$$

This completes the proof. \square

According to Cauchy's integral formula and Lemma 3.1, we have for sufficiently small h

$$\mathbf{U}(\zeta) = \frac{1}{2\pi i} \int_{\Gamma} K(\lambda) (\Delta(\zeta)/h - \lambda \mathbf{E}_m)^{-1} \mathbf{G}(\zeta) d\lambda = K(\Delta(\zeta)/h) \mathbf{G}(\zeta),$$

where $\mathbf{U}(\zeta) := \sum_{n=0}^{\infty} \mathbf{U}_n \zeta^n$, $\mathbf{U}_n := ((K(\partial_t^h)g)(t_1^n) \cdots (K(\partial_t^h)g)(t_m^n))^T$ and $(K(\partial_t^h)g)(t_i^n)$ denotes the approximation to $(K(\partial_t)g)(t_i^n)$. Then BGACQ is defined by

$$\mathbf{U}_n = \sum_{j=0}^n \mathbf{W}_j \mathbf{G}_{n-j}, \quad n = 0, 1, \dots, N,$$

where $K(\Delta(\zeta)/h) = \sum_{n=0}^{\infty} \mathbf{W}_n \zeta^n$. A direct calculation leads to

$$(K(\partial_t^h)g)(t_i^n) = \mathbf{e}_i^T \sum_{j=0}^n \mathbf{W}_j \mathbf{G}_{n-j}.$$

In this paper, we use the composite trapezoid rule to numerically compute the weight matrix \mathbf{W}_j , that is,

$$\mathbf{W}_j = \frac{1}{2\pi i} \int_{|\zeta|=\rho} K(\Delta(\zeta)/h) \zeta^{-j-1} d\zeta \approx \frac{\rho^{-j}}{L} \sum_{l=0}^{L-1} K(\Delta(\rho e^{il2\pi/L})/h) e^{-ijl2\pi/L},$$

where $\rho = \text{tol}^{1/6N}$, $L = 5N$ and $\text{tol} = 10^{-16}$. To achieve efficient computation, the above summations are implemented using the fast Fourier transform. In order to evaluate the matrix function $K(\Delta(\rho e^{il2\pi/L})/h)$, we first compute the invertible matrix \mathbf{P} and the diagonal matrix $\text{diag}(d_1, \dots, d_m)$ to diagonalize the matrix $\Delta(\rho e^{il2\pi/L})$, that is,

$$\Delta(\rho e^{il2\pi/L}) = \mathbf{P} \text{diag}(d_1, \dots, d_m) \mathbf{P}^{-1}.$$

Then $K(\Delta(\rho e^{il2\pi/L})/h)$ is evaluated by

$$K(\Delta(\rho e^{il2\pi/L})/h) = \mathbf{P} \text{diag}(K(d_1/h), \dots, K(d_m/h)) \mathbf{P}^{-1}.$$

We have performed numerical computations of $\Delta(\rho e^{il2\pi/L})$ for several BGAs satisfying Assumption 2.1. The results show that all these approaches lead to diagonalizable matrices. Furthermore, the condition numbers of the eigenvalues of $\Delta(\rho e^{il2\pi/L})$ are numerically found to be between one and two, indicating that the computations are not severely affected by instabilities. However, evaluating $K(\Delta(\rho e^{il2\pi/L})/h)$ introduces rounding errors of order $\mathcal{O}(h^{-1})$.

Let us turn to investigate the convergence property of BGACQ as the step size h of the coarse grid \mathcal{X}_N tends to 0, while the parameters k_1, k_2, m remain fixed. Following [20], we achieve this by integrating the product of the error bound for BGA and $K(\lambda)$ over the curve Γ . For $n = 0, \dots, N-1$, we have

$$(3.4) \quad (\mathbf{L} - h\mathbf{A}) \mathbf{Y}_n^{ref} = (h\lambda \mathbf{a} - \mathbf{l}) \mathbf{e}_m^T \mathbf{Y}_{n-1}^{ref} + h\mathbf{a} \mathbf{e}_m^T \mathbf{G}_{n-1} + h\mathbf{A} \mathbf{G}_n + \mathbf{Q}_n,$$

where $\mathbf{Q}_n = (q_1^n \cdots q_m^n)^T$. Combining Eqs. (2.5) and (3.4) yields

$$(\mathbf{L} - h\lambda \mathbf{A})(\mathbf{Y}_n^{ref} - \mathbf{Y}_n) = (h\lambda \mathbf{a} - \mathbf{l}) \mathbf{e}_m^T (\mathbf{Y}_{n-1}^{ref} - \mathbf{Y}_{n-1}) + \mathbf{Q}_n.$$

Denoting the collocation error $\epsilon_j^n := y(t_j^n) - y_j^n$ with $j = 1, \dots, m$, we obtain

$$\epsilon_m^n = \mathbf{R}_m(h\lambda)\epsilon_m^{n-1} + \mathbf{e}_m^T(\mathbf{L} - h\lambda\mathbf{A})^{-1}\mathbf{Q}_n.$$

An iterative calculation results in

$$\epsilon_m^n = \sum_{j=0}^n (\mathbf{R}_m(h\lambda))^j \mathbf{e}_m^T(\mathbf{L} - h\lambda\mathbf{A})^{-1}\mathbf{Q}_{n-j}.$$

By leveraging the representation of the collocation errors of BGA for IVP (1.5), we establish the convergence order of BGACQ for CI (1.2) when $\mu < 0$.

THEOREM 3.2. *Suppose that*

- *The function g in CI (1.2) possesses a continuous derivative of at least order $k_1 + k_2 + 2$ over $[0, T]$ and additionally satisfies the initial condition*

$$g(0) = g^{(1)}(0) = \dots = g^{(k_1+k_2+1)}(0) = 0;$$

- *The underlying ODE solver, BGA, satisfies Assumption 2.1;*
- *$K(\lambda)$ is analytic in the half-plane \mathbb{C}_σ and bounded as $|K(\lambda)| \leq M|\lambda|^\mu$ with a positive constant M and a negative real number μ .*

Then, for sufficiently large N and any n satisfying $0 \leq n \leq N - 1$, it follows that

$$\|\mathbf{Err}_{n,N}^{\text{CQ}}\| \leq Ch^{k_1+k_2+2}.$$

where

$$\mathbf{Err}_{n,N}^{\text{CQ}} := ((K(\partial_t)g)(t_1^n) - (K(\partial_t^h)g)(t_1^n), \dots, (K(\partial_t)g)(t_m^n) - (K(\partial_t^h)g)(t_m^n))^T.$$

Proof. Let us split the curve Γ into three parts,

$$\Gamma_1 := \{\lambda \in \Gamma : |\lambda| \leq 1\}, \Gamma_2 := \{\lambda \in \Gamma : h \leq |h\lambda| \leq 1\}, \Gamma_3 := \{\lambda \in \Gamma : |h\lambda| \geq 1\}.$$

For sufficiently small h , Lemma 2.1 guarantees

$$\|\mathbf{Q}_{n-j}\| \leq Ch^{k_1+k_2+3} \quad \text{for any } \lambda \in \Gamma_1.$$

Moreover, since 0 is not an eigenvalue of $\mathbf{A}^{-1}\mathbf{L}$, $\|\mathbf{e}_m^T(\mathbf{L} - h\lambda\mathbf{A})^{-1}\|$ remains bounded by C . Applying BGA to $y'(t) = \lambda y(t)$ with the initial value $y(0) = 1$ yields

$$(3.5) \quad \mathbf{R}_m(h\lambda) = e^{h\lambda} + \mathcal{O}((h\lambda)^{k_1+k_2+3}) \quad \text{as } h\lambda \rightarrow 0.$$

As a result, we have $|\mathbf{R}_m(h\lambda)|^j$ is bounded by C when $\lambda \in \Gamma_1$ and h is sufficiently small. Therefore, it follows

$$(3.6) \quad \left| \int_{\Gamma_1} K(\lambda)\epsilon_m^n d\lambda \right| \leq Ch^{k_1+k_2+2}.$$

Let's now consider the case where $\lambda \in \Gamma_2$. Combining Eq. (3.5) with Assumption 2.1 gives

$$\frac{|z|(1 - |\mathbf{R}_m(z)|^{n+1})}{1 - |\mathbf{R}_m(z)|} \leq C \quad \text{for } |z| \leq 1.$$

Additionally, $\|\mathbf{e}_m^T(\mathbf{L} - h\lambda\mathbf{A})^{-1}\|$ remains bounded by C . With the help of Lemma 2.1, we have

$$\begin{aligned}
\left| \int_{\Gamma_2} K(\lambda) \epsilon_m^n d\lambda \right| &\leq \int_{\Gamma_2} |K(\lambda)| \frac{1 - |\mathbf{R}_m(h\lambda)|^{n+1}}{1 - |\mathbf{R}_m(h\lambda)|} \|\mathbf{e}_m^T(\mathbf{L} - h\lambda\mathbf{A})^{-1}\| \|\mathbf{Q}_{n-j}\| |d\lambda| \\
&\leq Ch^{k_1+k_2+2} \int_{h\Gamma_2} |K(w/h)| |w|^{-1} \frac{|w|(1 - |\mathbf{R}_m(w)|^{n+1})}{1 - |\mathbf{R}_m(w)|} |dw| \\
(3.7) \quad &\leq Ch^{k_1+k_2+2-\mu}(1 + h^\mu) \leq Ch^{k_1+k_2+2}.
\end{aligned}$$

where the variable transformation $w = h\lambda$ is employed. In the case of $\lambda \in \Gamma_3$, it follows that $|\mathbf{R}_m(h\lambda)| \leq \rho < 1$, which implies $\sum_{j=0}^n |\mathbf{R}_m(h\lambda)|^j$ remains bounded by C . Meanwhile, we have the product $\|(\mathbf{L} - h\lambda\mathbf{A})^{-1}\| |h\lambda|$ is also bounded by C . Following Lemma 2.1, this implies that

$$\begin{aligned}
\left| \int_{\Gamma_3} K(\lambda) \epsilon_m^n d\lambda \right| &\leq C \int_{\Gamma_3} \frac{|\lambda|^\mu}{|h\lambda|} \left(\sum_{j=0}^n |\mathbf{R}_m(h\lambda)|^j \right) (\|(\mathbf{L} - h\lambda\mathbf{A})^{-1}\| |h\lambda|) \|\mathbf{Q}_{n-j}\| |d\lambda| \\
(3.8) \quad &\leq Ch^{k_1+k_2+2} \int_{\Gamma_3} |\lambda|^{\mu-1} |d\lambda| \leq Ch^{k_1+k_2+2-\mu}
\end{aligned}$$

Combining Eqs. (3.6), (3.7) and (3.8) gives

$$|(K(\partial_t)g)(t_m^n) - (K(\partial_t^h)g)(t_m^n)| \leq Ch^{k_1+k_2+2}.$$

Letting $\mathbf{R}_j(z) = \mathbf{e}_j^T(\mathbf{L} - z\mathbf{A})^{-1}(z\mathbf{a} - \mathbf{1})$, it follows by direct computation

$$\begin{aligned}
\epsilon_j^n &= \frac{\mathbf{R}_j(h\lambda)}{\mathbf{R}_m(h\lambda)} \mathbf{R}_m(h\lambda) \epsilon_m^{n-1} + \mathbf{e}_j^T(\mathbf{L} - h\lambda\mathbf{A})^{-1} \mathbf{Q}_n \\
&= \frac{\mathbf{R}_j(h\lambda)}{\mathbf{R}_m(h\lambda)} \sum_{j=1}^n (\mathbf{R}_m(h\lambda))^j \mathbf{e}_m^T(\mathbf{L} - h\lambda\mathbf{A})^{-1} \mathbf{Q}_{n-j} + \mathbf{e}_j^T(\mathbf{L} - h\lambda\mathbf{A})^{-1} \mathbf{Q}_n.
\end{aligned}$$

Since the ratio $\mathbf{R}_j(h\lambda)/\mathbf{R}_m(h\lambda)$ remains bounded by C for any $\lambda \in \Gamma$, we deduce that the convergence orders of the numerical errors on the fine grids coincide with those on the coarse grids. This implies that the convergence of BGACQ is uniform across the entire grid, that is,

$$\|\mathbf{Err}_{n,N}^{\text{CQ}}\| \leq Ch^{k_1+k_2+2}.$$

This completes the proof. \square

In the case of $\mu \geq 0$, we define r to be the smallest integer exceeding μ , and let $K_r(\lambda) = K(\lambda)/\lambda^r$. It follows by a direct calculation that

$$\begin{aligned}
(K(\partial_t)g)(t_i^n) - (K(\partial_t^h)g)(t_i^n) &= (K_r(\partial_t)(\partial_t)^r g)(t_i^n) - (K_r(\partial_t^h)(\partial_t)^r g)(t_i^n) \\
&\quad + (K(\partial_t^h)(\partial_t^h)^{-r}(\partial_t)^r g)(t_i^n) - (K(\partial_t^h)g)(t_i^n).
\end{aligned}$$

Suppose that g satisfies

$$g(0) = g^{(1)}(0) = \dots = g^{(r+k_1+k_2+1)}(0) = 0.$$

By application of Theorem 3.2, we have that

$$(3.9) \quad |(K_r(\partial_t)(\partial_t)^r g)(t_i^n) - (K_r(\partial_t^h)(\partial_t)^r g)(t_i^n)| \leq Ch^{k_1+k_2+2}.$$

Note that

$$K(\Delta(\zeta)/h) = \frac{1}{2\pi i} \int_{\Gamma'} K(\lambda/h)(\Delta(\zeta) - \lambda \mathbf{E}_m)^{-1} d\lambda,$$

where Γ' comprise a circular arc $|\lambda| = r$ and $\operatorname{Re}(\lambda) \geq h\sigma$ such that it falls in the stability domain of the ODE solver. Based on Lemma 3.1, we obtain the following derivation

$$\sum_{n=0}^N \|\mathbf{W}_n\| \leq C \int_{\Gamma'} |K(\lambda/h)| \sum_{n=0}^N |\mathbf{R}_m(\lambda)|^n |d\lambda|.$$

Split Γ' into two parts,

$$\Gamma'_1 := \{\lambda \in \Gamma' : |\lambda| \leq h\} \quad \text{and} \quad \Gamma'_2 := \Gamma' \setminus \Gamma'_1.$$

Then we can obtain the result using an analogous argument to the proof of Theorem 3.2

$$\int_{\Gamma'_1} |K(\lambda/h)| \sum_{n=0}^N |\mathbf{R}_m(\lambda)|^n |d\lambda| \leq C,$$

and

$$\begin{aligned} \int_{\Gamma'_2} |K(\lambda/h)| \sum_{n=0}^N |\mathbf{R}_m(\lambda)|^n |d\lambda| &= \int_{\Gamma'_2} |K(\lambda/h)| |\lambda|^{-1} \left(|\lambda| \sum_{n=0}^N |\mathbf{R}_m(\lambda)|^n \right) |d\lambda| \\ &\leq Ch^{-\mu} \int_{\Gamma'_2} |\lambda|^{\mu-1} |d\lambda| \leq C \begin{cases} |\log(h)|, & \mu = 0, \\ h^{-\mu}, & \mu > 0. \end{cases} \end{aligned}$$

Therefore, we get

$$(3.10) \quad \sum_{n=0}^N \|\mathbf{W}_n\| \leq C \begin{cases} |\log(h)|, & \mu = 0, \\ h^{-\mu}, & \mu > 0. \end{cases}$$

The difference $((\partial_t^h)^{-r}(\partial_t)^r g)(t) - g(t)$ is just the local error of BGA applied to ODE $y^{(r)}(t) = g^{(r)}(t)$ with zero initial values (see [2]). Thus we have

$$|((\partial_t^h)^{-r}(\partial_t)^r g - g)(t_i^n)| \leq Ch^{k_1+k_2+3}.$$

Letting $\delta \mathbf{G}_n := (((\partial_t^h)^{-r}(\partial_t)^r g - g)(t_1^n), \dots, ((\partial_t^h)^{-r}(\partial_t)^r g - g)(t_m^n))^T$, we get

$$(3.11) \quad \begin{aligned} &|(K(\partial_t^h)(\partial_t^h)^{-r}(\partial_t)^r g)(t_i^n) - (K(\partial_t^h)g)(t_i^n)| \\ &\leq \|\mathbf{e}_i^T\| \sum_{j=0}^n \|\mathbf{W}_{n-j}\| \|\delta \mathbf{G}_j\| \leq C \begin{cases} h^{k_1+k_2+3} |\log(h)|, & \mu = 0, \\ h^{k_1+k_2+3-\mu}, & \mu > 0. \end{cases} \end{aligned}$$

Now we get the convergence property of BGACQ by combining Eqs. (3.9) and (3.11) in the case of $\mu \geq 0$.

THEOREM 3.3. *Suppose that*

- *The function g in CI (1.2) possesses a continuous derivative of at least order $r + k_1 + k_2 + 2$ over $[0, T]$ and additionally satisfies the initial condition*

$$g(0) = g^{(1)}(0) = \dots = g^{(r+k_1+k_2+1)}(0) = 0,$$

where r denotes the smallest integer exceeding μ ;

- The underlying ODE solver, BGA, satisfies Assumption 2.1;
- $K(\lambda)$ is analytic in the half-plane \mathbb{C}_σ and bounded as $|K(\lambda)| \leq M|\lambda|^\mu$ with a positive constant M and a nonnegative real number μ .

Then, for sufficiently large N and any n satisfying $0 \leq n \leq N - 1$, it follows that

$$\|\mathbf{Err}_{n,N}^{\text{CQ}}\| \leq Ch^{\min\{k_1+k_2+3-\mu, k_1+k_2+2\}}.$$

In solving time-domain boundary integral equations for some acoustic scattering problems, the dissipative property of CQ becomes critical. Lower dissipation in these methods generally translates to improved computational efficiency. As discussed for RKCQ in [5, Chapter 5], discretizing the time-domain boundary integral equation using BGACQ involves replacing the free-space Green's function kernel $\mathcal{G}(\mathbf{x}, \lambda)$ with $\mathcal{G}(\mathbf{x}, \hat{\lambda})$. Here, for sufficiently small $\hat{\lambda}h$, $\hat{\lambda}$ is the solution of $\mathbf{R}_m(\hat{\lambda}h) = e^{\lambda h}$. Analyzing the numerical scheme's dissipation then involves expanding $\mathbf{R}_m^{-1}(e^{-i\omega})$ to obtain the approximation $\hat{\lambda}$ to the frequency $\lambda = i\omega$. Since

$$\mathbf{R}'_m(z) = \mathbf{e}_m^T((\mathbf{L} - z\mathbf{A})^{-1}\mathbf{A}(\mathbf{L} - z\mathbf{A})^{-1})(z\mathbf{a} - \mathbf{1}) + \mathbf{e}_m^T(\mathbf{L} - z\mathbf{A})^{-1}\mathbf{a},$$

we have $\mathbf{R}'_m(0) = \mathbf{e}_m^T\mathbf{L}^{-1}(-\mathbf{A}\mathbf{L}^{-1}\mathbf{1} + \mathbf{a}) = 1$, which implies the inverse \mathbf{R}_m^{-1} around origin is well-defined. We have computed the difference between λ and $\hat{\lambda}$ numerically for various BGACQs, and present the results in the following,

$$\begin{aligned} \text{BGACQ}_{0,1}^3 &: \hat{\lambda} = \lambda + 5.1 \times 10^{-4}\omega(\omega h)^3 + 7.6 \times 10^{-4}i\omega(\omega h)^4 + \omega\mathcal{O}((\omega h)^5), \\ \text{BGACQ}_{0,2}^4 &: \hat{\lambda} = \lambda - 6.2 \times 10^{-5}i\omega(\omega h)^4 + 6.7 \times 10^{-5}\omega(\omega h)^5 + \omega\mathcal{O}((\omega h)^6), \\ \text{BGACQ}_{1,2}^5 &: \hat{\lambda} = \lambda + 4.9 \times 10^{-7}\omega(\omega h)^5 - 8.8 \times 10^{-8}i\omega(\omega h)^6 + \omega\mathcal{O}((\omega h)^7), \\ \text{BGACQ}_{0,1}^{12} &: \hat{\lambda} = \lambda + 2.0 \times 10^{-5}\omega(\omega h)^3 + 2.1 \times 10^{-5}i\omega(\omega h)^4 + \omega\mathcal{O}((\omega h)^5), \\ \text{BGACQ}_{0,2}^{12} &: \hat{\lambda} = \lambda - 1.1 \times 10^{-6}i\omega(\omega h)^4 + 1.2 \times 10^{-6}\omega(\omega h)^5 + \omega\mathcal{O}((\omega h)^6), \\ \text{BGACQ}_{1,2}^{12} &: \hat{\lambda} = \lambda - 2.0 \times 10^{-8}\omega(\omega h)^5 - 2.0 \times 10^{-8}i\omega(\omega h)^6 + \omega\mathcal{O}((\omega h)^7). \end{aligned}$$

We can see the dissipation of BGACQ is demonstrably small and diminishes further as the block size increases.

If the initial conditions for g in Theorems 3.2 and 3.3 are not met, the convergence order of BGACQ will be reduced. To overcome this limitation, modifications to BGACQ should be explored. We first focus on the case with $\mu < 0$. For a general g , applying Taylor's expansion yields

$$\begin{aligned} g(t) &= \sum_{l=0}^{k_1+k_2+1} \frac{t^l}{l!} g^{(l)}(0) + \frac{1}{(k_1+k_2+1)!} \int_0^t g^{(k_1+k_2+2)}(s)(t-s)^{k_1+k_2+1} ds \\ &= \sum_{l=0}^{k_1+k_2+1} \frac{g^{(l)}(0)}{l!} p_l(t) + \tilde{p}(t), \end{aligned}$$

where

$$p_l(t) := t^l, \quad \tilde{p}(t) := \frac{1}{(k_1+k_2+1)!} \int_0^t g^{(k_1+k_2+2)}(s)(t-s)^{k_1+k_2+1} ds.$$

We solve the following equations for $i = 1, \dots, m$ and $l = 0, \dots, k_1+k_2+1$,

$$(3.12) \quad (K(\partial_t)p_l)(t_i^n) = \mathbf{e}_i^T \sum_{j=0}^n \mathbf{W}_{n-j} \mathbf{p}_l^j + \sum_{j=0}^{k_1+k_2+1} \omega_{i,j}^n p_l(t_j^0),$$

where $\mathbf{p}_l^j := (p_l(t_1^j), \dots, p_l(t_m^j))^T$. Letting

$$\mathbf{w}_i := \begin{pmatrix} w_{i,0}^n \\ w_{i,1}^n \\ \vdots \\ w_{i,k_1+k_2+1}^n \end{pmatrix}, \mathbf{K}_i := \begin{pmatrix} (K(\partial_t)p_0)(t_i^n) \\ (K(\partial_t)p_1)(t_i^n) \\ \vdots \\ (K(\partial_t)p_{k_1+k_2+1})(t_i^n) \end{pmatrix},$$

$$\mathbf{V} := \begin{pmatrix} p_0(t_0^0) & p_0(t_1^0) & \cdots & p_0(t_{k_1+k_2+1}^0) \\ p_1(t_0^0) & p_1(t_1^0) & \cdots & p_1(t_{k_1+k_2+1}^0) \\ \vdots & \vdots & & \vdots \\ p_{k_1+k_2+1}(t_0^0) & p_{k_1+k_2+1}(t_1^0) & \cdots & p_{k_1+k_2+1}(t_{k_1+k_2+1}^0) \end{pmatrix},$$

Eq. (3.12) reduces to

$$\mathbf{V}\mathbf{w}_i = \mathbf{K}_i - \begin{pmatrix} \mathbf{e}_i^T \sum_{j=0}^n \mathbf{W}_{n-j} \mathbf{P}_0^j \\ \vdots \\ \mathbf{e}_i^T \sum_{j=0}^n \mathbf{W}_{n-j} \mathbf{P}_{k_1+k_2+1}^j \end{pmatrix}.$$

Following a similar derivation as for Eq. (3.10), we obtain

$$\sum_{j=0}^n \|\mathbf{W}_{n-j}\| \leq C \text{ for } \mu < 0 \text{ as } h \rightarrow 0.$$

Since $(K(\partial_t)p_l)(t_i^n) = \mathcal{O}(h^l)$ and $p_l(t_j^0) = \mathcal{O}(h^l)$, it follows that $\|\mathbf{w}_i\| = \mathcal{O}(1)$. Then we define the modified BGACQ (MBGACQ) by

$$(K(\bar{\partial}_t^h)g)(t_i^n) := (K(\partial_t^h)g)(t_i^n) + \mathbf{w}_i^T \hat{\mathbf{G}}_0,$$

where $\hat{\mathbf{G}}_0 := (g(t_0^0), \dots, g(t_{k_1+k_2+1}^0))^T$. We can now express the quadrature error as

$$\begin{aligned} (K(\bar{\partial}_t^h)g)(t_i^n) - (K(\partial_t)g)(t_i^n) &= (K(\bar{\partial}_t^h)\tilde{p})(t_i^n) - (K(\partial_t)\tilde{p})(t_i^n) \\ &= (K(\partial_t^h)\tilde{p})(t_i^n) - (K(\partial_t)\tilde{p})(t_i^n) + \mathbf{w}_i^T \hat{\mathbf{p}}_0, \end{aligned}$$

where $\hat{\mathbf{p}}_0 := (\tilde{p}(t_0^0), \dots, \tilde{p}(t_{k_1+k_2+1}^0))^T$. Because $\|\hat{\mathbf{p}}_0\| = \mathcal{O}(h^{k_1+k_2+2})$ as $h \rightarrow 0$ and $\tilde{p}(t)$ satisfies the initial condition in Theorem 3.2, both $(K(\partial_t^h)\tilde{p})(t_i^n) - (K(\partial_t)\tilde{p})(t_i^n)$ and $\mathbf{w}_i^T \hat{\mathbf{p}}_0$ are $\mathcal{O}(h^{k_1+k_2+2})$. This implies that MBGACQ recovers the full convergence order. For the case of $\mu \geq 0$, the initial condition $g(0) = \dots = g^{(r)}(0)$ ensures the well-posedness of CI, and the convergence order of MBGACQ can be derived similarly to the case of $\mu < 0$.

4. Numerical Experiments. In this section, we present several numerical examples to validate the theoretical properties of BGACQ for calculation of CI (1.2). For this purpose, we compute the maximum of quadrature errors, $\|\mathbf{Err}_{n,N}^{\text{CQ}}\|$, in the n -th block of BGACQ. Furthermore, we numerically compute the convergence order, denoted by ‘‘Order’’, for the errors in each block. The formula used is

$$\text{Order} := \left| \frac{\log \|\mathbf{Err}_{n,N_1}^{\text{CQ}}\| - \log \|\mathbf{Err}_{n,N_2}^{\text{CQ}}\|}{\log N_1 - \log N_2} \right|.$$

TABLE 4.1

Maximum norms, $\|\mathbf{Err}_{N-1,N}^{\text{CQ}}\|$, of absolute errors of $\text{BGACQ}_{0,1}^3$ applied to Example 1 with $\mu < 0$.

N	$\mu = -0.2$		$\mu = -0.8$		$\mu = -1.8$	
	$\ \mathbf{Err}_{N-1,N}^{\text{CQ}}\ $	Order	$\ \mathbf{Err}_{N-1,N}^{\text{CQ}}\ $	Order	$\ \mathbf{Err}_{N-1,N}^{\text{CQ}}\ $	Order
2^3	2.8×10^{-4}	–	1.1×10^{-4}	–	9.8×10^{-6}	–
2^4	3.1×10^{-5}	3.2	1.3×10^{-5}	3.1	5.3×10^{-7}	4.2
2^5	3.8×10^{-6}	3.1	1.5×10^{-6}	3.1	5.0×10^{-8}	3.4
2^6	4.6×10^{-7}	3.0	1.8×10^{-7}	3.0	5.3×10^{-9}	3.2
2^7	5.7×10^{-8}	3.0	2.2×10^{-8}	3.0	6.2×10^{-10}	3.1
2^8	7.0×10^{-9}	3.0	2.7×10^{-9}	3.0	7.9×10^{-11}	3.0

TABLE 4.2

Maximum norms, $\|\mathbf{Err}_{N-1,N}^{\text{CQ}}\|$, of absolute errors of $\text{BGACQ}_{0,1}^3$ applied to Example 1 with $\mu \geq 0$.

N	$\mu = 0$		$\mu = 0.8$		$\mu = 1.8$	
	$\ \mathbf{Err}_{N-1,N}^{\text{CQ}}\ $	Order	$\ \mathbf{Err}_{N-1,N}^{\text{CQ}}\ $	Order	$\ \mathbf{Err}_{N-1,N}^{\text{CQ}}\ $	Order
2^3	3.6×10^{-4}	–	1.2×10^{-3}	–	4.3×10^{-2}	–
2^4	3.7×10^{-5}	3.3	1.2×10^{-4}	3.3	5.6×10^{-3}	2.9
2^5	4.3×10^{-6}	3.1	1.6×10^{-5}	2.8	9.6×10^{-4}	2.6
2^6	5.2×10^{-7}	3.0	2.1×10^{-6}	2.9	1.9×10^{-4}	2.4
2^7	6.4×10^{-8}	3.0	2.6×10^{-7}	3.0	4.3×10^{-5}	2.1
2^8	7.9×10^{-9}	3.0	3.2×10^{-8}	3.1	9.1×10^{-6}	2.2

The first two examples demonstrate the convergence rates established in Theorems 3.2 and 3.3. The third example assess the stability of BGACQ by numerically solving a class of integral equations with rapidly varying and conservative solutions. Finally, we consider the calculation of a family of oscillatory integrals.

EXAMPLE 1. We compute CI (1.2) using $\text{BGACQ}_{0,1}^3$, where the Laplace transform of its kernel is

$$K_\mu(\lambda) = \frac{\lambda^\mu}{1 - e^{-\lambda}}.$$

The expression for this family of CIs can be derived as follows,

$$(K_\mu(\partial_t)g)(t) = \sum_{j=0}^{\infty} (\partial_t^\mu g)(t-j) \quad \text{with} \quad (\partial_t^\mu g)(t) = \frac{1}{\Gamma(\mu)} \int_0^t (t-s)^{-\mu-1} g(s) ds.$$

We select $g(t) = e^{-0.4t} \sin^6 t$ to satisfy the initial conditions in Theorems 3.2 and 3.3 for the case where $\mu \leq 2$. Due to the difficulty of directly computing the exact value, we employ the value obtained using $\text{BGACQ}_{0,1}^3$ with 2^{10} blocks as a reference value.

Table 4.1 presents the computed results for the case of $\mu < 0$. As expected from Theorem 3.2, the observed convergence order is approximately 3, which aligns well with the theoretical findings. Table 4.2 summarizes the numerical results for $\mu \geq 0$. We observe a computed convergence order of 3 for $\text{BGACQ}_{0,1}^3$ when $\mu = 0$ or 0.8. This aligns with the theoretical prediction in Theorem 3.3. For the case where $\mu = 1.8$, the computed order is $4 - \mu = 2.2$, again consistent with the theoretical estimation in Theorem 3.3.

CQs have proven valuable tools for computing fractional derivatives and integrals. The following example explores the application of the proposed BGACQ to the

TABLE 4.3

Maximum norms, $\|\mathbf{Err}_{N-1,N}^{\text{CQ}}\|$, of absolute errors computed by $\text{MBGACQ}_{k_1,k_2}^{m*}$ for CI (4.1) with $\alpha = 0.5$.

N	$(k_1, k_2) = (0, 1)$		$(k_1, k_2) = (0, 2)$		$(k_1, k_2) = (1, 2)$	
	$\ \mathbf{Err}_{N-1,N}^{\text{CQ}}\ $	Order	$\ \mathbf{Err}_{N-1,N}^{\text{CQ}}\ $	Order	$\ \mathbf{Err}_{N-1,N}^{\text{CQ}}\ $	Order
8	1.2×10^{-2}	–	7.3×10^{-4}	–	1.3×10^{-6}	–
24	3.4×10^{-4}	3.2	8.9×10^{-6}	4.0	1.1×10^{-8}	4.4
40	6.7×10^{-5}	3.2	1.1×10^{-6}	4.0	8.0×10^{-10}	5.1
56	2.3×10^{-5}	3.1	3.0×10^{-7}	4.0	1.4×10^{-10}	5.1
72	1.1×10^{-5}	3.1	1.1×10^{-7}	4.0	3.8×10^{-11}	5.2

TABLE 4.4

Maximum norms, $\|\mathbf{Err}_{N-1,N}^{\text{CQ}}\|$, of absolute errors computed by $\text{MBGACQ}_{k_1,k_2}^{m*}$ for CI (4.1) with $\alpha = 0.9$.

N	$(k_1, k_2) = (0, 1)$		$(k_1, k_2) = (0, 2)$		$(k_1, k_2) = (1, 2)$	
	$\ \mathbf{Err}_{N-1,N}^{\text{CQ}}\ $	Order	$\ \mathbf{Err}_{N-1,N}^{\text{CQ}}\ $	Order	$\ \mathbf{Err}_{N-1,N}^{\text{CQ}}\ $	Order
8	1.5×10^{-2}	–	1.3×10^{-3}	–	1.7×10^{-6}	–
24	4.3×10^{-4}	3.2	1.5×10^{-5}	4.0	1.7×10^{-8}	4.2
40	8.7×10^{-5}	3.1	2.0×10^{-6}	4.0	1.5×10^{-9}	4.8
56	3.0×10^{-5}	3.1	5.1×10^{-7}	4.0	2.9×10^{-10}	4.9
72	1.4×10^{-5}	3.1	1.9×10^{-7}	4.0	8.0×10^{-11}	5.1

calculation of fractional integrals, demonstrating its effectiveness in this specific area.

EXAMPLE 2. Consider calculation of CI in the form of

$$(4.1) \quad \frac{1}{\Gamma(\alpha)} \int_0^t (t-s)^{\alpha-1} (\sin(s)+1)e^{0.8s} ds \quad \text{with } t \in [0, 5] \text{ and } \alpha \in (0, 1).$$

Since the function $(\sin(s)+1)e^{0.8s}$ does not vanish at $s = 0$, we utilize $\text{MBGACQ}_{0,1}^3$, $\text{MBGACQ}_{0,2}^4$, and $\text{MBGACQ}_{1,2}^5$ to compute CI (4.1) and verify the predicted convergence order. As shown in Tables 4.3 ($\alpha = 0.5$) and 4.4 ($\alpha = 0.9$), the computed convergence orders are approximately 3, 4, 5, respectively, which aligns with the theoretical expectations established in Theorem 3.2. To elucidate the key difference between $\text{BGACQ}_{1,2}^5$ and $\text{MBGACQ}_{1,2}^5$, Figure 4.1 compares their absolute errors on the total grid for varying values of N . We observe that the correction term incorporated in $\text{MBGACQ}_{1,2}^5$ significantly reduces the numerical errors around $t = 0$.

Now let us test the stability of the proposed CQ by solving an integral equation with a fast varying and conservative solution.

EXAMPLE 3. Solve the integral equation

$$(4.2) \quad \int_0^t k(t-s)u(s)ds = g(t) \quad \text{with } t \in [0, 4].$$

Here the Laplace transform of $k(t)$ is selected to be $K(\lambda) = 1 - e^{-\lambda}$ and $g(t) = e^{-100(t-0.5)^2}$. Its exact solution is $u(t) = \sum_{j=0}^3 g(t-j)$ (see [5]). Since direct calculations indicate that both $u(t)$ and its derivatives are negligible at $t = 0$, the correction term is omitted in the implementation of CQs for this case.

For comparison purposes, we employ various CQs to solve Eq. (4.2), including BDF2CQ, TRCQ, $\text{BGACQ}_{0,1}^3$, $\text{BGACQ}_{0,2}^4$, and $\text{BGACQ}_{1,2}^5$, k -stage Lobatto IIIC

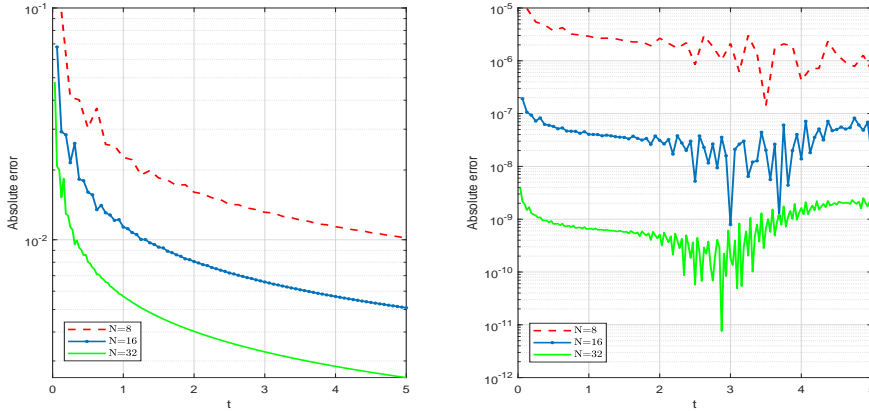


FIG. 4.1. Comparison between pointwise errors of $BGACQ_{1,2}^5$ (left) and $MBGACQ_{1,2}^5$ (right) for CI (4.1) with $\alpha = 0.5$ and various N .

RKCQ ($LRKCQ_k$) and k -stage Gauss RKCQ ($GRKCQ_k$) with $k = 3, 4, 5$. All approaches utilize a total of 120 quadrature nodes. Consequently, the 3-stage, 4-stage and 5-stage methods use 40, 30 and 24 blocks, respectively. Computed results are shown in Figure 4.2. The first subfigure of Figure 4.2 demonstrates that BDF2CQ suffers from significant departure from the true solution due to its strong dissipative nature. While TRCQ is inherently conservative, its accuracy is also compromised in this case by an insufficiently small time step size. While BGACQ exhibits a slower convergence rate compared to LRKCQ and GRKCQ with the same stage, the second and third subfigures in Figure 4.2 reveal that BGACQ's damping errors lie between LRKCQ and GRKCQ, suggesting GRKCQ's efficiency across the compared schemes. Notably, with increasing convergence order of CQs (see the fourth subfigure), the damping becomes negligible. Our numerical experiments have also identified several conservative BGACQs, such as $BGACQ_{1,1}^4$, that achieve numerical accuracy comparable to the conservative $GRKCQ_4$. Figure 4.3 compares $BGACQ_{1,1}^4$ with $GRKCQ_4$, demonstrating that the difference in numerical results computed by these methods is insignificant, while a significant damping effect is observed for $BGACQ_{0,2}^4$ in the third subfigure of Figure 4.2. However, analyzing the convergence properties of these conservative BGACQs remains an open challenge for future research.

While conservative CQs offer advantages in certain scenarios, dissipative CQs can demonstrate superior performance for specific problems. Here, we illustrate the benefits of dissipative CQs by applying them to the following problem.

EXAMPLE 4. Consider calculation of the oscillatory integral with a fast decaying integrand

$$(4.3) \quad \int_0^2 J_0(\omega(2-s))e^{-10s} \frac{s^6}{1+25s^2} ds.$$

Here J_0 denotes the first-kind Bessel function of order 0. Its Laplace transform is $(\omega^2 + \lambda^2)^{-1/2}$, which is singular at $\lambda = \pm i\omega$. As $\omega \rightarrow \infty$, the problem becomes increasingly hyperbolic.

We employ the 4-stage methods, $GRKCQ_4$, $BGACQ_{1,1}^4$ and $BGACQ_{0,2}^4$, to compute CI (4.3). The relative errors, presented in Figure 4.4, demonstrate that the

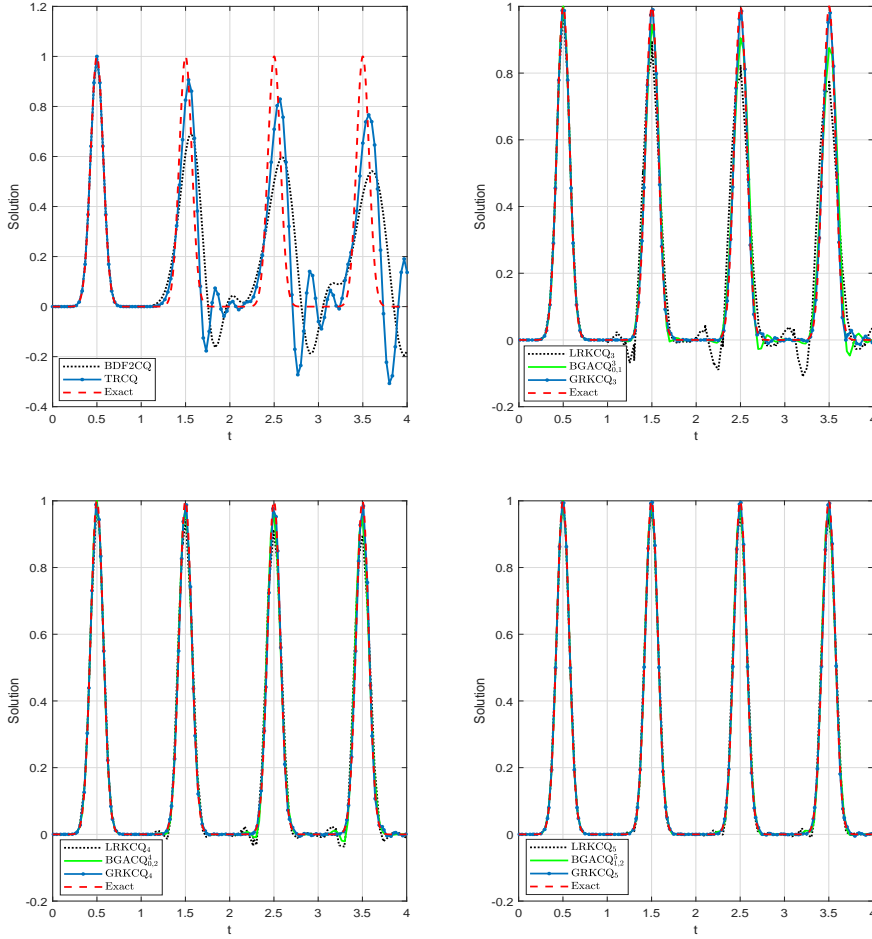


FIG. 4.2. Comparison of numerical solutions computed by CQs for Eq. (4.2) with 120 quadrature nodes.

dissipative CQ (BGACQ $_{0,2}^4$) consistently outperforms the two conservative methods regardless of an increase in either the quadrature nodes or the oscillation parameter ω . This superiority can be attributed, in part, to the faster decay of the dissipative CQ's stability function near the imaginary axis compared to the conservative CQs. This faster decay allows the dissipative CQ to significantly mitigate rounding errors.

5. Conclusions. This paper explores a family of BGACQs for calculation of CI (1.2) with a hyperbolic kernel. These quadrature rules can be understood as modifications of LMCQs or RKCQs. Notably, BGACQs are implemented on the uniform grid and offer the advantage of adjustable convergence rates without requiring additional grid points. Furthermore, when coupled with an ODE solver satisfying Assumption 2.1, BGACQs demonstrate high-order accuracy and effectiveness in solving a wide range of hyperbolic problems. Their inherent flexibility suggests significant potential for diverse numerical applications, including fractional differential equations, time-domain boundary integral equations, Volterra integral equations, and potentially

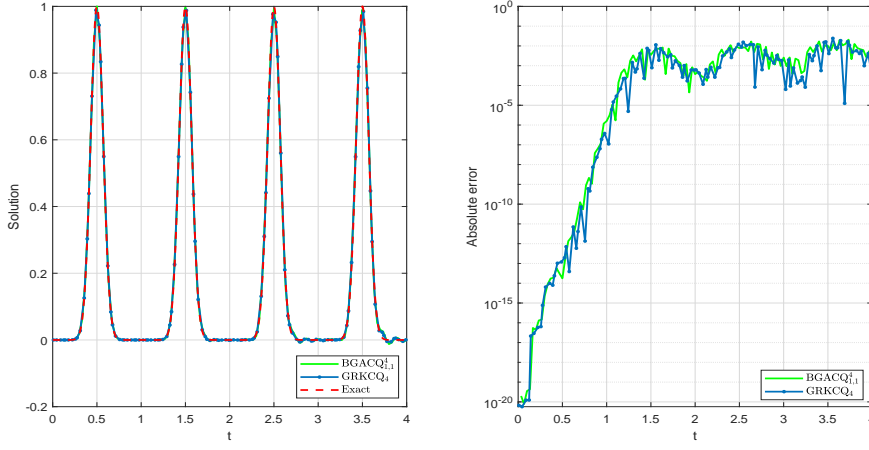


FIG. 4.3. Comparison of numerical solutions computed by $BGACQ_{1,1}^4$ and $GRKCQ_4$ for Eq. (4.2) with 120 quadrature nodes.

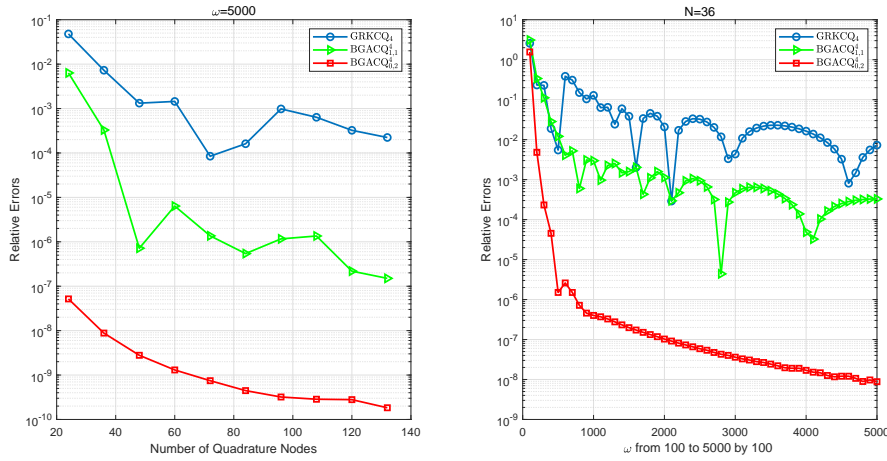


FIG. 4.4. Comparison of dissipative and conservative CQs for CI (4.3). The left part shows the relative errors as the quadrature nodes increase. The right part shows the relative errors as ω increases.

many more.

While this paper focuses on BGACQs with small block sizes, higher-order schemes or capturing global information necessitate larger block sizes, leading to a significant increase in computational cost. Fast algorithms for calculation of quadrature weights, as explored in [19], offer a potential remedy. This challenge is also crucial for developing a varying-stepsize version of BGACQs.

Acknowledgements. We express our sincere gratitude to anonymous reviewers for their insightful comments, which significantly enhanced the quality of our paper.

REFERENCES

- [1] L. Banjai, *Multistep and multistage convolution quadrature for the wave equation: algorithms and experiments*, SIAM J. Sci. Comput., 32(2010), pp.2964–2994.
- [2] L. Banjai and C. Lubich, *An error analysis of Runge-Kutta convolution quadrature*, BIT Numer. Math., 51(2011), pp.483–496.
- [3] L. Banjai and M. Kachanovska, *Fast convolution quadrature for the wave equation in three dimensions*, J. Comput. Phys., 279(2014), pp.103–126.
- [4] L. Banjai and M. López-Fernández, *Efficient high order algorithms for fractional integrals and fractional differential equations*, Numer. Math. 141 (2019), pp.289–317.
- [5] L. Banjai and F. Sayas, *Integral Equation Methods for Evolutionary PDE: A Convolution Quadrature Approach*, Springer Nature, 2022.
- [6] L. Banjai and M. Ferrari, *Runge-Kutta convolution quadrature based on Gauss methods*, arXiv preprint, arXiv:2212.07170, 2022.
- [7] L. Banjai and M. Ferrari, *Generalized convolution quadrature based on the trapezoidal rule*, arXiv preprint, arXiv:2305.11134, 2023.
- [8] L. Brugnano and D. Trigiante, *Solving Differential Equations by Multistep Initial and Boundary Value Methods*, Gordon and Breach Science Publisher, 1998.
- [9] H. Brunner, *Collocation Methods for Volterra Integral and Related Functional Differential Equations*, Cambridge University Press, 2004.
- [10] H. Brunner, *Volterra Integral Equations: An Introduction to Theory and Applications*, Cambridge University Press, 2017.
- [11] E. Cuesta, C. Lubich and C. Palencia, *Convolution quadrature time discretization of fractional diffusion-wave equations*, Math. Comp., 75(2006), pp.673–696.
- [12] P. Davies and D. Duncan, *Convolution-in-time approximations of time domain boundary integral equations*, SIAM J. Sci. Comput., 35(2013), pp.43–61.
- [13] H. Eruslu and F. Sayas, *Polynomially bounded error estimates for trapezoidal rule convolution quadrature*, Comput. Math. Appl., 79(2020), pp.1634–1643.
- [14] M. Fischer, *Fast and parallel Runge-Kutta approximation of fractional evolution equations*, SIAM J. Sci. Comput., 41(2019), pp.927–947.
- [15] F. Iavernaro and F. Mazzia, *Solving ordinary differential equations by generalized Adams methods: properties and implementation techniques*, Appl. Numer. Math., 28(1998), pp.107–126.
- [16] F. Iavernaro and F. Mazzia, *Block-boundary value methods for the solution of ordinary differential equations*, SIAM J. Sci. Comput., 21(1999), pp.323–339.
- [17] B. Jin, B. Li and Z. Zhou, *Correction of high-order BDF convolution quadrature for fractional evolution equations*, SIAM J. Sci. Comput., 39(2017), pp.3129–3152.
- [18] M. López-Fernández and S. Sauter, *Generalized convolution quadrature with variable time stepping*, IMA J. Numer. Anal., 33(2013), pp.1156–1175.
- [19] M. López-Fernández and S. Sauter, *Generalized convolution quadrature based on Runge-Kutta methods*, Numer. Math., 133(2016), pp.743–779.
- [20] C. Lubich, *Convolution quadrature and discretized operational calculus I*, Numer. Math., 52(1988), pp.129–145.
- [21] C. Lubich, *Convolution quadrature and discretized operational calculus II*, Numer. Math., 52(1988), pp.413–425.
- [22] C. Lubich and A. Ostermann, *Runge-Kutta methods for parabolic equations and convolution quadrature*, Math. Comp., 60(1993), pp.105–131.
- [23] C. Lubich, *Convolution quadrature revisited*, BIT Numer. Math., 44(2004), pp.503–514.
- [24] J. Melenk and A. Rieder, *On superconvergence of Runge-Kutta convolution quadrature for the wave equation*, Numer. Math., 147(2021), pp.157–188.
- [25] J. Nick, B. Kovács and C. Lubich, *Time-dependent electromagnetic scattering from thin layers*, Numer. Math., 150(2022), pp.1123–1164.
- [26] H. Ren, J. Ma and H. Liu, *A convolution quadrature using derivatives and its application*, BIT Numer. Math., 64(2024), pp.1–23.
- [27] A. Rieder, F. Sayas and J. Melenk, *Time domain boundary integral equations and convolution quadrature for scattering by composite media*, Math. Comp., 91(2022), pp.2165–2195.
- [28] J. Shi and M. Chen, *High-order BDF convolution quadrature for subdiffusion models with a singular source term*, SIAM J. Numer. Anal., 61(2023), pp.2559–2579.
- [29] E. Stein, *Harmonic Analysis: Real-Variable Methods, Orthogonality, and Oscillatory Integrals*, Princeton University Press, Princeton, 1993.
- [30] X. Wang, R. Wildman, D. Weile and P. Monk, *A finite difference delay modeling approach to the discretization of the time domain integral equations of electromagnetics*, IEEE Trans. Antennas Propag., 56(2008), pp.2442–2452.

- [31] K. Xu, A. Austin and K. Wei, *A fast algorithm for the convolution of functions with compact support using Fourier extensions*, SIAM J. Sci. Comput., 39(2017), pp.3089–3106.
- [32] K. Xu and F. Loureiro, *Spectral approximation of convolution operators*, SIAM J. Sci. Comput., 40(2018), pp.2336–2355.